PHYSICAL REVIEW A VOLUME 40, NUMBER 4 AUGUST 15, 1989

Near-threshold behavior of multimode continuous-wave dye lasers with amplitude-modulated pump

Stephen H. Chakmakjian, Stephanos Papademetriou, Karl Koch, and C. R. Stroud, Jr.
The Institute of Optics, University of Rochester, Rochester, New York 14627
(Received 13 March 1989)

We use amplitude-modulation techniques to investigate the response of a multimode dye laser when its pump intensity is sinusoidally amplitude modulated. A theoretical model is presented based on a Floquet analysis to obtain the stationary-state first-harmonic response of the population inversion and that of the laser intensity as a function of modulation frequency. We perform experiments in multimode continuous-wave dye lasers to demonstrate the validity of this theory in describing the behavior of multimode lasers operating near the lasing threshold.

I. INTRODUCTION

Noise in laser systems can be characterized as being of two general types: multiplicative and additive. The dominant source of additive noise is spontaneous-emission fluctuations, while multiplicative noise arises from loss or gain fluctuations. In this paper we will study the effects of multiplicative fluctuations on the amplitude stability of lasers.

The dynamics of a single-mode laser with multiplicative fluctuations can be very different from those of a laser with purely additive noise.[1–12] Early evidence of this fact came from studies of the statistical properties of lasers with multiplicative noise. These differences are quantified by measurements of the normalized variance of the laser intensity near threshold,[1] the distribution of the laser intensity near threshold,[1–3] and the first-passage-time distribution of a two-mode laser.[4–6] These statistical studies emphasized the importance of the effects of multiplicative fluctuations in lasers.

Instead of studying the statistical behavior of a laser system, the effects of pump fluctuations can be characterized, in part, by examining the power spectrum of the fluctuations of the laser intensity. Yu *et al.*[13] measure the power spectrum of the intensity of an argon-pumped single-mode cw dye laser. The intensity of the laser behaves as a low-pass amplifier to the amplitude fluctuations of the pump. Furthermore, the bandwidth of the fluctuations of the laser intensity decreases as the intensity of the pump is reduced to the threshold value. This intensity-dependent bandwidth is a good example of critical slowing down in a nonlinear system operating near a critical point. Similar behavior has been predicted in an electrically pumped solid-state laser with current noise. Agrawal and Roy[14] show that at high intensities, the power spectrum of the intensity of a semiconductor laser is affected by current noise in the pumping mechanism. The bandwidth of the intensity noise spectrum of a laser is determined by a systematic time constant that depends on the intracavity intensity.

Yet another approach to studying the effects of pump fluctuations on a laser system is to provide an external modulation of the pump and monitor the response of the laser. The problem was theoretically treated by Mandel and co-workers[15–17] and others.[18,19] They predict a delayed bifurcation as a control parameter is swept through a critical point. Scharpf *et al.*[20] explore the response of an argon-ion laser to a linear ramp in the intracavity loss. The laser undergoes a delayed bifurcation as the loss is varied through threshold. Papoff *et al.*[21] performed an experiment studying the delayed bifurcation with square-wave modulation of the loss. The mean switching time increases as a control parameter is brought near a period-doubling bifurcation point. These experiments demonstrate the usefulness of modulating the gain or the loss of a laser to study non-steady-state laser dynamics.

These studies have concentrated on the dynamics of single-mode lasers. To date, little attention has been given to multimode systems. Also, most treatments have concentrated on the laser intensity, while the atomic behavior has often been eliminated from the dynamics. In this paper, we address both problems by examining the response of the total intensity and the atomic inversion in multimode lasers subjected to multiplicative fluctuations. We calculate the response of a single-mode laser to a sinusoidally modulated pump. Expressions for the first-harmonic response of the laser intensity and the excited-state population of the laser transition are derived. We compare these theoretical predictions with experiments in multimode cw dye-laser systems. Amplitude-modulation (AM) spectroscopy is used to study the near-threshold dynamics of these lasers. This form of spectroscopy has been used to probe the absorption spectrum of strongly driven atoms.[22–26] In our experiment we modulate the intensity of the pump beam and study the total intensity of the laser and the intensity of the fluorescence from the gain medium (the fluorescent intensity is proportional to the excited-state population). We perform a phase-sensitive measurement of the modulations induced in the laser and the fluorescent intensities using a lock-in amplifier. The modulation frequency is varied to obtain a spectrum of the laser's response. We perform a quantitative comparison of a multimode experiment with single-mode laser theory and find good agreement. These

spectral measurements are applied in a novel scheme to measure the laser-cavity lifetime.

II. THEORY

The modulation frequencies used in our experiments are much smaller than the frequency separation between the cavity modes. Our measurements average the response over a time long compared with the period of the intermodal beat note. Consequently, we have chosen to employ a rate-equation model that concentrates on the total intensity of the laser but ignores the dynamics occurring at the intermodal beat frequency. This treatment is identical to a single-mode laser model.

We start with a four-level rate-equation model where the equations of motion for the upper pump level and the lower lasing level have been adiabatically eliminated, since the population decay rates from these levels are rapid. After these approximations are made, the atomic inversion is equal to the excited-state population. We begin the theoretical treatment with the equations of motion for the population of the upper laser level ρ, for a four-level laser medium

$$\frac{d}{dt}\rho=-\frac{1}{T_1}(1+I_p+I)\rho+\frac{I_p}{T_1}\ , \tag{1}$$

and the rate equation for the dimensionless intensity of the laser I,

$$\frac{d}{dt}I=\left[g\rho-\frac{1}{\tau_c}\right]I\ . \tag{2}$$

The dimensionless intensity of the laser is defined as the rate of stimulated emission times the excited-state population lifetime T_1. The dimensionless intensity of the pump is I_p (the dimensionless intensity of the pump is the pump rate times T_1), the passive-cavity lifetime is τ_c, and the gain is given by

$$g=\frac{\alpha c}{L}\ , \tag{3}$$

where α is the integrated absorption coefficient (i.e., the gain per pass) of the interaction region of the gain medium, L is the length of the cavity, and c is the speed of light. Recently, a more accurate model for the material dynamics of dye lasers has been developed. Fu and Haken[27,28] have developed a band model which takes into account the multilevel structure of the dye molecule. However, we find that simple four-level rate equations are adequate to describe the dynamics observed in our experiments.

Setting the time derivatives in Eqs. (1) and (2) equal to zero, we solve for the steady-state response of the excited-state population and the laser intensity. Setting the time derivative to zero in Eq. (2) yields the steady-state value for the excited-state population

$$\rho_{ss}=\frac{1}{g\tau_c}\ , \tag{4}$$

and setting the time derivative in Eq. (1) to zero yields the steady-state solution for the laser intensity

$$I_{ss}=\frac{I_p}{I_{thr}}-1\ , \tag{5}$$

where we have introduced the threshold pump intensity I_{thr} given by

$$I_{thr}=\frac{1}{g\tau_c-1}\ . \tag{6}$$

The equalities in Eqs. (4) and (5) are valid for $I_p \geq I_{thr}$. We have ignored the solutions that are unstable above threshold (i.e., the off solutions). The steady-state solution for the excited-state population when the laser is on is independent of the pump intensity I_p. This phenomenon is known as inversion clamping.[29] Once threshold has been reached, additional pump power is converted into laser light [see Eq. (5)]. We will investigate gain or inversion clamping using AM spectroscopy to study the response of the excited-state population to a fluctuating pump intensity.

From here on we will not be concerned with a steady-state analysis but instead we will be analyzing the temporal response of the laser by modulating the pump intensity $I_p(t)$ and observing the response of the laser intensity $I(t)$ and the excited-state population $\rho(t)$ to the modulated pump. The pump intensity $I_p(t)$ is weakly modulated at the angular frequency $\delta\omega$ as

$$I_p(t)=\bar{I}_p+2\delta I_p\cos(\delta\omega t)\ . \tag{7}$$

The dc or time-averaged pump intensity is represented by $\bar{I}_p$, and the amplitude of the modulation sidebands is represented by δI_p, which is considered small in this experiment. The modulation frequency $\delta\omega$ is expressed in units of radians per second. Floquet's theorem tells us that in the stationary state, the excited-state population and the laser intensity will respond at higher harmonics of the modulation fundamental $\delta\omega$. Since we are interested in the stationary-state response, we can expand the temporal response of these variables in a harmonic series of overtones of $\delta\omega$. The excited-state population can be written as

$$\rho(t)=\sum_{n=-\infty}^{\infty}\rho_n\exp(in\delta\omega t)\ , \tag{8a}$$

and the intensity of the laser is given by

$$I(t)=\sum_{n=-\infty}^{\infty}I_n\exp(in\delta\omega t)\ . \tag{8b}$$

The nth-harmonic response of the excited-state population is ρ_n, and the nth-harmonic response of the laser intensity is I_n. When we substitute Eqs. (8a) and (8b) into Eqs. (1) and (2) and equate terms of equal time dependence, we get the following recurrence relation:

$$\begin{aligned}(1+\bar{I}_p+in\delta\omega T_1)\rho_n &= -\sum_{m=-\infty}^{\infty}\rho_m I_{n-m}-\delta I_p(\rho_{n+1}+\rho_{n-1})+\bar{I}_p\delta_{n,0}\\ &\quad+\delta I_p(\delta_{n,1}+\delta_{n,-1})\ ,\end{aligned} \tag{9}$$

from the excited-state population rate equation, Eq. (1), and

$$(1+in\delta\omega\tau_c)I_n=g\tau_c\sum_{m=-\infty}^{\infty}\rho_m I_{n-m}\ , \tag{10}$$

from the intensity rate equation, Eq. (2), where $\delta_{i,j}$ is the Kronecker delta function.

We can analyze these recurrence relations for a particular value of the subscript n to obtain the nth-harmonic response of $I(t)$ and $\rho(t)$. Since we use weak modulation in this experiment, we can truncate the harmonic expansions of the excited-state population and the intensity of the laser to first order ($n=1$). Likewise, we ignore all products which are of order higher than 1 (i.e., neglect terms such as $\delta I_p\rho_1$ and $\rho_1 I_1$). With these simplifications, we get four recurrence relations: two from the excited-state population recurrence relation, Eq. (9) for $n=0$ and $n=1$; and two from the intensity recurrence relation, Eq. (10). For the index $n=0$ we recover the steady-state solutions we obtained without the modulation (i.e., $\rho_0=\rho_{ss}$ and $I_0=I_{ss}$). This result is consistent with the perturbative approach we are using. Solving Eqs. (9) and (10) for $n=1$, we get the first-harmonic response of the intensity of the laser,

$$I_1=I_0\left[\frac{1}{\rho_0}-1\right]\delta I_p\frac{[I_0-(\delta\omega T_1)(\delta\omega\tau_c)]-i[(1+\bar{I}_p+I_0)(\delta\omega\tau_c)]}{[(1+\bar{I}_p+I_0)(\delta\omega\tau_c)]^2+[I_0-(\delta\omega T_1)(\delta\omega\tau_c)]^2}\ . \tag{11}$$

The time-averaged responses of the intensity and the excited-state population are I_0 and ρ_0, respectively.

The first-harmonic response of the excited-state population can be solved in a similar manner, and the result is

$$\rho_1=(1-\rho_0)(\delta\omega\tau_c)\delta I_p\frac{[(1+\bar{I}_p+I_0)(\delta\omega\tau_c)]+i[I_0-(\delta\omega T_1)(\delta\omega\tau_c)]}{[(1+\bar{I}_p+I_0)(\delta\omega\tau_c)]^2+[I_0-(\delta\omega T_1)(\delta\omega\tau_c)]^2}\ . \tag{12}$$

To understand this phenomenon better, we plot the response of the intensity of the laser and of the excited-state population on the same plot in Fig. 1. In this figure the population lifetime is one-tenth the cavity lifetime $T_1=0.1\tau_c$, and the amount above threshold is 10%, or $I_0=0.1$. The first thing to notice is that the response of the laser and the population cross each other at the half-maximum values for each. The population response is a high-pass filter for fluctuations the laser cannot follow. Furthermore, in this limit where $(\delta\omega T_1)(\delta\omega\tau_c)\ll I_0$, the response of the intensity of the laser to a modulated pump intensity is a Lorentzian whose half-width at half maximum (HWHM) is equal to the reciprocal of the cavity lifetime times the pump parameter β, which we define as

$$\beta=\frac{I_0}{1+I_0+\bar{I}_p}\ . \tag{13a}$$

In the parameter regime of our experiment, the laser and pump intensities are nonsaturating (i.e., $I_0,\bar{I}_p\ll 1$); consequently, the pump parameter is equal to the fractional amount above threshold, or

$$\beta\simeq I_0=\frac{\bar{I}_p}{I_{\rm thr}}-1\ . \tag{13b}$$

The response of the excited-state population displays a dip at low modulation frequency. We consider this result to be a manifestation of the effects of inversion clamping at nonzero frequencies. Another way to interpret this result is that the laser acts as a pump-intensity noise eater, keeping the inversion of the atoms constant in the presence of low-frequency fluctuations.

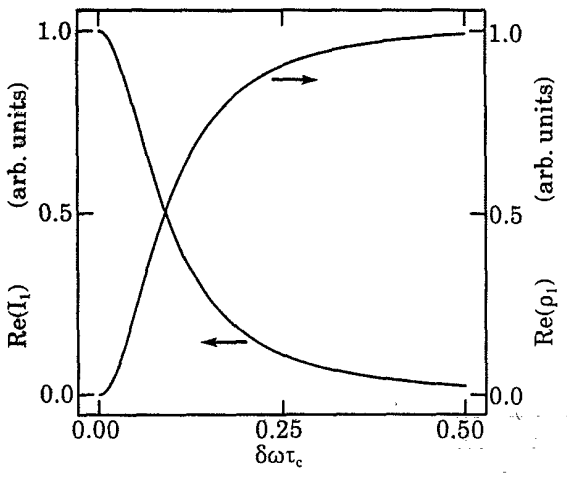

FIG. 1. The in-phase first-harmonic response of the laser intensity I_1 and the excited-state population ρ_1 vs the normalized pump modulation frequency $\delta\omega\tau_c$. The parameters used in this figure are $T_1=0.1\tau_c$, and $I_0=0.1$ (i.e., the laser is 10% above threshold).

III. EXPERIMENTAL SETUP

We have carried out an experiment to test these theoretical predictions in multimode lasers. In our experiment we measure the spectrum of the near-threshold dynamic behavior of the intensity and excited-state population for several different dye-laser cavity configurations. In this section, we will discuss the experimental procedures and techniques we use to make these measurements. A diagram of the experimental apparatus is shown in Fig. 2. We study standing-wave and ring-laser cavities. In all cavities we use two 5-cm-radius high reflectors to focus and recollimate the laser through the gain medium. A knife-edge high-reflector mirror is used in all cavities to allow the argon pump beam to be brought in parallel to the cavity axis (see Fig. 2). In the case of the high-Q cavities, we use a fourth high reflector

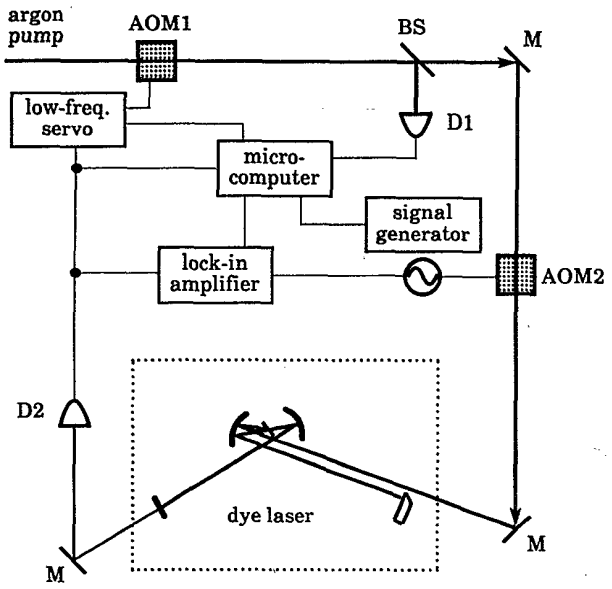

FIG. 2. Experimental setup. The following labeling conventions are used in this figure: AOM1—acousto-optic modulator for servo circuit; AOM2—acousto-optic modulator for modulating the pump; BS—beam splitter; M—mirror; D1—detector for measuring argon-pump beam intensity; D2—detector for measuring dye-laser intensity.

in the cavities; otherwise, a 5% output coupler is used. No dispersive elements are used in any of the cavities. Furthermore, we verify, using a Fabry-Pérot interferometer, that the time-averaged spectrum of the lasers always consists of many longitudinal modes. In fact, for the higher pump settings the time-averaged spectrum consisted of hundreds of modes.

The crucial problem in doing near-threshold studies is keeping the laser at a fixed amount above threshold. This is difficult, since small fluctuations in the intensity of the pump or in the threshold can cause full-scale fluctuations in the intensity of the laser. We can overcome this problem by using a closed-loop-servo circuit to hold the intensity of the dye laser fixed during our measurements. The servo makes small adjustments in the intensity of the pump beam to maintain a constant dye-laser intensity. The intensity of the pump beam is adjusted with an acousto-optic modulator (AOM1 in Fig. 2), which diffracts a variable amount of power out of the beam. As long as the threshold fluctuations are small, this technique allows us to keep the laser at a fixed fraction above threshold merely by controlling the output intensity of the dye laser. If the fluctuations in the in the cavity loss are large, then the slope efficiency changes appreciably and the intensity of the laser is not a good indicator of the amount the laser is operating above threshold. The bandwidth of the servo was kept below 100 Hz so that it would not overlap with frequencies used in the modulation experiment. The servo circuit has an external offset to allow the computer to control the intensity of the dye laser.

We use a second acousto-optic modulator (AOM2 in Fig. 2) to weakly modulate the intensity of the pump beam during the modulation experiment. Since we collect data with the pump intensity only 1% above the threshold value, it is necessary to keep the modulation depth to less than 0.1% of the argon total intensity. We adjust the modulation depth of the argon intensity to ensure that the modulation detected in the intensity of the dye laser is less than one-tenth of the total time-averaged dye-laser intensity (i.e., $I_1 \leq I_0/10$) for the minimum pump setting in the experiment. A sine wave is supplied to AOM2 by a voltage-controlled oscillator, which is controlled by our computer. The zeroth-order diffracted beam from AOM2 is used to pump the dye lasers, except for the high-Q cavities. In the case of the high-Q cavities, both ring and standing wave, we pump the laser with the first-order diffracted beam from AOM2. We use the first-order diffracted beam of AOM2 to rapidly extinguish the pump intensity so that we can directly measure the cavity lifetime of the high-Q cavities (the lifetime of the cavities with output couplers is too short to measure in this manner) by monitoring the decay of the intensity of the laser. The first-order diffracted beam from an AOM can be turned off completely whereas the zeroth-order beam cannot.

To compare the experiment with the theory, it is necessary to accurately measure the intensity of the pump at each setting, as well as the intensity of the pump at threshold. To determine the threshold intensity, we measure the intensity of the dye laser and the intensity of the pump beam at several values near threshold and extrapolate to zero dye-laser intensity to find the intensity of the pump at threshold. We use the computer and the external offset to the servo for this slope-efficiency measurement. The computer ramps the intensity of the dye laser and at each setting records both the intensity of the dye laser and the pump (see detectors D1 and D2 in Fig. 2). These slope-efficiency data are also used in determining the intensity of the pump during the experiment. We use the intensity of the dye laser divided by the slope of the laser-intensity versus pump-intensity plot to determine the intensity of the pump rather than directly measuring the intensity of the pump at each setting. We assume a linear relation between dye-laser intensity and pump intensity. In this manner, we eliminate most of the error resulting from any drift of the lasing threshold during the experiment. This method is efficacious if the threshold fluctuations are small and the slope efficiency does not change.

For each cavity configuration, we perform a slope-efficiency measurement for the laser. Then we set the dye-laser intensity to one of several equally spaced values near threshold and record the dye-laser intensity at that setting. While the laser intensity is held fixed by the servo circuit and AOM1, we vary the modulation frequency driving the AOM2. The signal from the photo diode monitoring the laser intensity is fed into a dual-phase lock-in amplifier. The lock-in measures the magnitude and sign of the in-phase and in-quadrature components of the amplitude modulation in the intensity of the dye laser. The computer records both the in-phase and the in-quadrature signal from the lock-in at each frequency setting. The dye-laser intensity is then set to a new value

and another frequency sweep is performed. After recording a series of dye-laser spectra, we switch the input signal to the lock-in to record spectra of the intensity of the fluorescence. We image the fluorescence from the interaction region of the laser onto a pinhole detector. We choose the f number of the lens to effectively resolve the 10 μm diameter by 100-μm-long interaction region in the dye jet. We are careful to detect light only from the center of the interaction region to ensure that the atoms are within the mode volume of the laser.

To compare these multimode experiments with single-mode theory, we fit our modulation data with the signal amplitude and the cavity lifetime as free parameters. For the high-Q cavities, both ring and standing wave, we compare the cavity lifetime, which yields the best fit to our modulation data, with the cavity lifetime we measure directly. The lifetimes of the high-Q cavities are greater than the 100-ns fall time of our modulation and detection systems. This enables us to turn off the pump fast enough to directly measure the exponential decay of the cavity. We can compare the cavity lifetime we measure directly with the lifetime obtained from fitting our data to single-mode theory (see Sec. IV A).

IV. DISCUSSION OF RESULTS

A. Multimode lasers and single-mode theory

In the first part of our experiment we show that single-mode traveling-wave theory gives an accurate description of the critical slowing down effects in the total intensity of multimode standing-wave and bidirectional ring lasers. We analyze high-Q cavities in which all the mirrors are high reflectors. The lifetimes of the cavities are maximized by extending the cavity length to 1 m for the standing-wave cavities and 2 m for the ring cavities. The free spectral range of these cavities is 150 MHz. These cavities typically have lifetimes τ_c on the order of 200–400 ns.

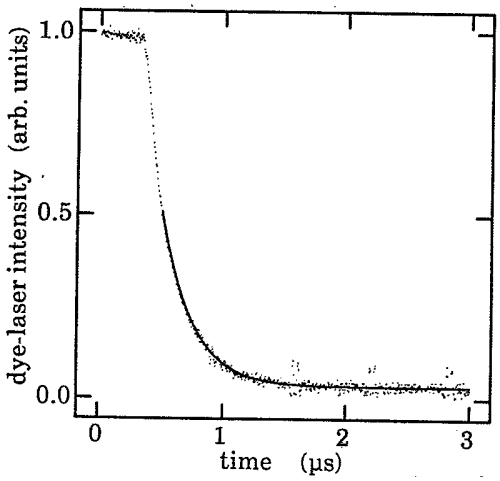

FIG. 3. Dye-laser intensity vs time for a multimode, high-Q standing-wave laser. This figure shows the decay of the dye-laser intensity after a rapid and complete turn off of the pump beam. The solid line represents the best-fit exponential whose time constant is 245 ns.

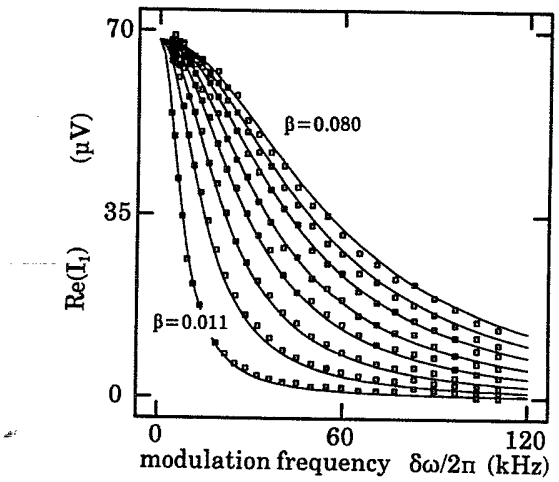

FIG. 4. The in-phase first-harmonic response of the laser intensity I_1 vs the pump modulation frequency $\delta\omega/2\pi$. We plot the in-phase or x-channel output of the lock-in amplifier vs frequency for a high-Q standing-wave laser for several values of the pump parameter β given in Eq. (13). The curves, from left to right, correspond to $\beta=0.011$, $\beta=0.021$, $\beta=0.031$, $\beta=0.041$, $\beta=0.050$, $\beta=0.060$, $\beta=0.070$, and $\beta=0.080$. The solid lines represent the single-mode best theoretical fit to all the data fit simultaneously. The cavity lifetime which gives this fit is 230 ns.

We will discuss the data for a high-Q standing-wave laser cavity first. In Fig. 3 we plot the dye-laser intensity as a function of time after the pump is extinguished. All data points are fit to an exponential, except those earlier than 100 ns after the start of the decay, since these times coincide with the turn-off time of the pump. This procedure ensures that the lifetime we measure is truly the

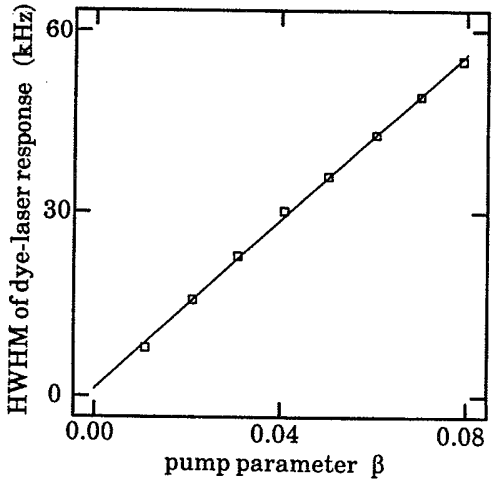

FIG. 5. The modulation bandwidth (HWHM) of the in-phase first-harmonic response of the intensity of the laser vs the pump parameter β. The curves shown in Fig. 4 were individually fit to Lorentzians and the bandwidth (HWHM) of these fits are plotted here with squares. The solid line represents the result of a linear regression performed on these points. The slope of this line is related to the reciprocal of the cavity lifetime $1/\tau_c$. The cavity lifetime we get from the slope is 235 ns.

passive-cavity lifetime and not an active-cavity lifetime. The solid line in Fig. 3 represents the best exponential fit of 245±4 ns to these data. We will compare this cavity lifetime with the lifetime we derive from fitting the AM spectra of the multimode dye laser to single-mode theory [see Eq. (11)]. In Fig. 4 we plot the voltage from the output of the lock-in amplifier (squares) versus modulation frequency $\delta\omega/2\pi$ for several different pump powers. This voltage corresponds to the in-phase first-harmonic response of the dye-laser intensity. The curves broaden as the pump parameter β is increased [see Eqs. (13a) and (13b)]. All modulation spectra shown in Fig. 4 are fit simultaneously using the time-averaged intensity I_0, which we measure directly before each modulation run, and the data points from the lock-in amplifier as constraints. The best theoretical fits using single-mode theory are also shown in Fig. 4 (solid lines). The cavity lifetime used to fit the data in Fig. 4 is 230 ns, which agrees with the lifetime we measure directly from the data in Fig. 3 to within 7%. This implies that single-mode theory is quite accurate in describing the behavior of the total intensity of a multimode standing-wave laser operating near threshold. Another way of analyzing the data is to separately fit the individual modulation spectra to Lorentzians and plot the HWHM of each file versus the measured pump parameter β. In Fig. 5 we plot the HWHM of the individual fits together with the best-fit straight line through the data. The reciprocal of the slope of this line is equal to 2π times the cavity lifetime τ_c. The value of the cavity lifetime we obtain from the slope is 235±3 ns, which is also in close agreement with the value obtained directly from the data shown in Fig. 3.

We have performed the same analysis on a high-Q bidirectional ring laser. For this case, we measure the total intensity exiting the ring cavity from one direction of travel. The exponential decay of the laser intensity is shown in Fig. 6. The exponential fit (solid line) corresponds to a lifetime of 329±4 ns. In Fig. 7 we plot the in-phase response of the total intensity in one direction of the multimode ring dye laser. The cavity lifetime which gives the best simultaneous fit to all these data using single-mode theory is 335 ns. In Fig. 8 we plot the HWHM of the individual fits to these data versus the pump parameter β, given in Eq. (13a). We perform a linear regression on these data to obtain a cavity lifetime

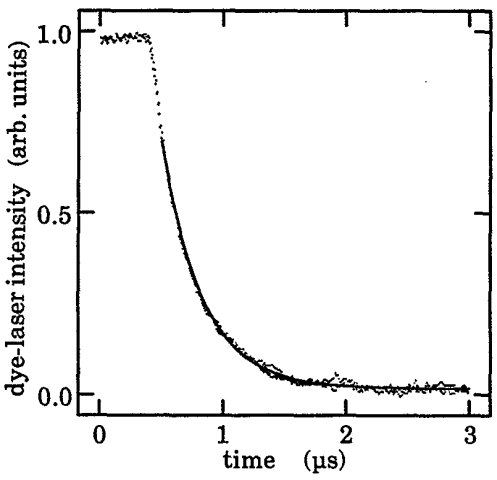

FIG. 6. Dye-laser intensity vs time for a multimode, high-Q bidirectional ring laser. This figure shows the decay of the dye-laser intensity in one direction of the ring laser after a rapid and complete turn off of the pump beam. The solid line represents the best-fit exponential whose time constant is 329 ns.

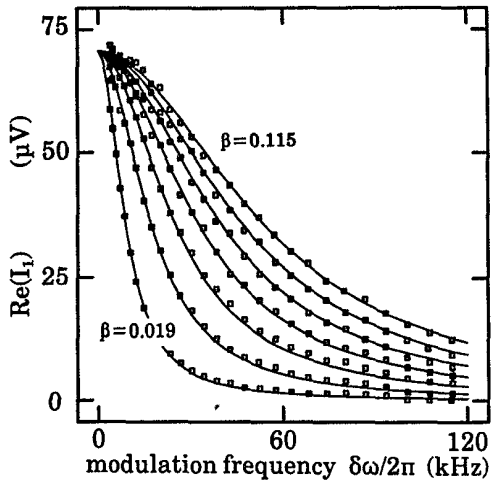

FIG. 7. The in-phase first-harmonic response of the laser intensity I_1 vs the pump modulation frequency $\delta\omega/2\pi$. We plot the in-phase or x-channel output of the lock-in amplifier vs frequency for a high-Q bidirectional ring laser for several values of the pump parameter β given in Eq. (13). The curves, from left to right, correspond to β=0.019, β=0.036, β=0.053, β=0.070, β=0.085, β=0.100, and β=0.115. The solid lines represent the single-mode best theoretical fit to all the data fit simultaneously. The cavity lifetime which gives us this fit is 335 ns.

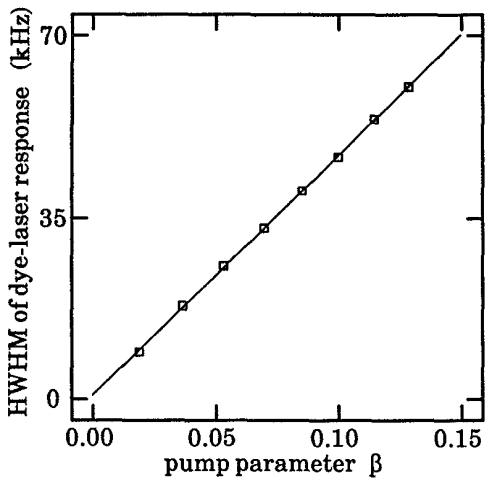

FIG. 8. The modulation bandwidth HWHM of the in-phase first-harmonic response of the intensity of the laser vs the pump parameter β. The curves shown in Fig. 7 were individually fit to Lorentzians and the bandwidth (HWHM) of these fits are plotted here with squares. The solid line represents a linear regression performed on these points. The slope of this line is related to the reciprocal of the cavity lifetime $1/\tau_c$. The cavity lifetime we get from the slope is 344 ns.

of 344±2 ns. This value for the lifetime is within 5% of the value obtained directly from the data shown in Fig. 6. We conclude that single-mode laser theory provides an adequate model for the behavior of the total intensity of multimode ring lasers as well as standing-wave lasers operating near threshold.

B. Laser intensity and fluorescent intensity

To connect the effects of critical slowing down in the dye-laser intensity with the effects observed in the fluorescent intensity, we have characterized both quantities for the same cavity configurations. In this section we will discuss the first-harmonic response of the intensity of the laser and the intensity of the fluorescence from the interaction region in the gain medium for a multimode standing-wave laser with a 5% output coupler. In Fig. 9 we plot the in-phase response of the fluorescent intensity to the modulated pump. To fit the fluorescence data we assume that the detector measures some fluorescence from atoms that are pumped by the argon beam but are not in the interaction region of the dye laser. A small dc offset is added to the theory to simulate this experimental complication. The solid lines correspond to a single-mode theoretical fit with a cavity lifetime of 87 ns. In Fig. 10 we plot the response of the laser intensity to the modulation of the pump. The single-mode theoretical fit to these data yields a cavity lifetime of 86 ns. This cavity lifetime corresponds quite well with that from fitting the response of the fluorescence. We conclude that the intensity of the fluorescence from the interaction region of the multimode laser behaves as the single-mode theory predicts. To better appreciate the relation between the response of the fluorescence intensity and the response of the laser intensity, we plot both responses versus the modulation frequency $\delta\omega/2\pi$ for the same pump parameter β, in Figs. 11(a) and 11(b). In Fig. 11(a) the in-phase response of the fluorescent intensity is plotted together with the in-phase response of the laser intensity versus the modulation frequency $\delta\omega/2\pi$. In Fig. 11(b) we plot the in-quadrature response of the intensity of the fluorescence and that of the intensity of the laser versus the modulation frequency $\delta\omega/2\pi$. The data in Figs. 11(a) and 11(b) show that when the dye laser can follow the modulations of the pump the atomic inversion is constant in time. However, at higher frequencies the laser cannot respond to fluctuations of the pump, so the inversion becomes unclamped and the atoms begin to respond to the modulations or fluctuations of the pump intensity.

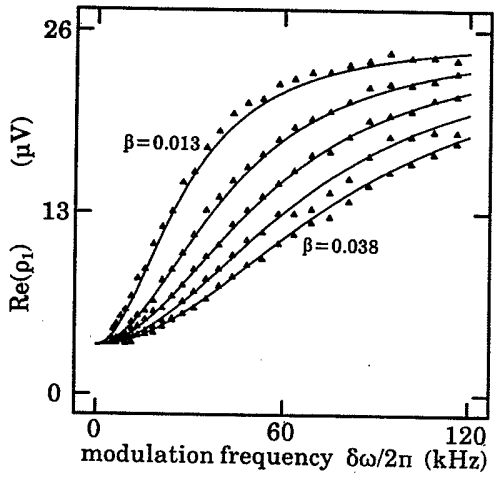

FIG. 9. The in-phase first-harmonic response of the intensity of the fluorescence from atoms in the interaction region of the gain medium vs the pump modulation frequency $\delta\omega/2\pi$. We plot the in-phase or x-channel output of the lock-in amplifier vs frequency for a standing-wave laser with a 5% output coupler for several values of the pump parameter β given in Eq. (13). The curves, from left to right, correspond to $\beta=0.013$, $\beta=0.019$, $\beta=0.026$, $\beta=0.033$, and $\beta=0.038$. The solid lines represent the single-mode best theoretical fit to all the data fit simultaneously. The cavity lifetime which gives us this fit is 87 ns.

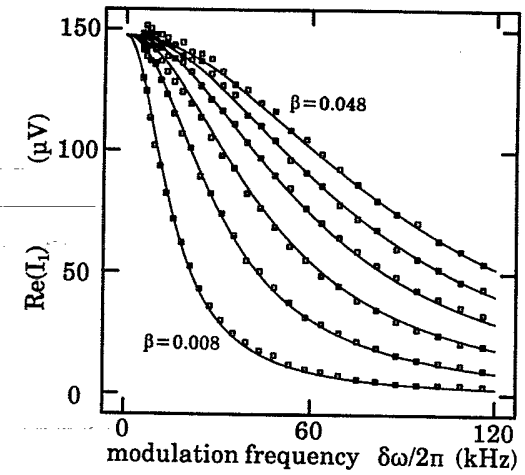

FIG. 10. The in-phase first-harmonic response of the laser intensity I_1 vs the pump modulation frequency $\delta\omega/2\pi$. We plot the in-phase or x-channel output of the lock-in amplifier vs frequency for a standing-wave laser with a 5% output coupler for several values of the pump parameter β given in Eq. (13). The curves, from left to right, correspond to $\beta=0.008$, $\beta=0.017$, $\beta=0.025$, $\beta=0.033$, $\beta=0.041$, and $\beta=0.048$. The solid lines represent the single-mode best theoretical fit to all the data fit simultaneously. The cavity lifetime which gives us this fit is 86 ns.

In Fig. 12 we plot the HWHM of the response of the laser intensity (squares) and the HWHM of the response of the fluorescent intensity (triangles) versus the pump parameter β. The half-widths of the fluorescent-intensity response and the half-widths of the laser-intensity response lie along the same line (see Fig. 12) with a slope corresponding to a cavity lifetime of 90 ns. The solid line in Fig. 12 represents the results of a linear regression analysis performed on all the data shown in the figure.

We collect data for multimode ring and standing-wave laser cavities for both high-Q cavities and cavities with a 5% output coupler. In Fig. 13 we plot the HWHM of the in-phase first-harmonic response of the fluorescent intensity and the laser intensity for three of the cavities we studied. The HWHM of the high-Q standing-wave-laser response ($\tau_c=246$ ns) and the high-Q ring-laser response

($\tau_c = 344$ ns) are labeled as (b) and (c), respectively, in Fig. 13. In these high-Q cavities the dominant loss mechanism is probably the imperfect Brewster reflection from the dye jet. In the standing-wave laser the modes encounter more surfaces per cavity round trip (the focusing mirrors and the dye jet are encountered twice per round trip); consequently, this cavity has a shorter lifetime than the high-Q ring of comparable length. The cavities with output couplers have approximately the same lifetime of 90 ns regardless of the configuration (ring or standing wave). The dominant loss mechanism in these cavities is undoubtedly the output coupler, which is encountered only once per cavity round trip for both the standing-wave and the ring cavities. The data labeled (a) in Fig. 13 are for a unidirectional ring laser with a 5% output coupler ($\tau_c = 85$ ns). The laser is forced to oscillate in one direction by retroreflecting the output from one direction

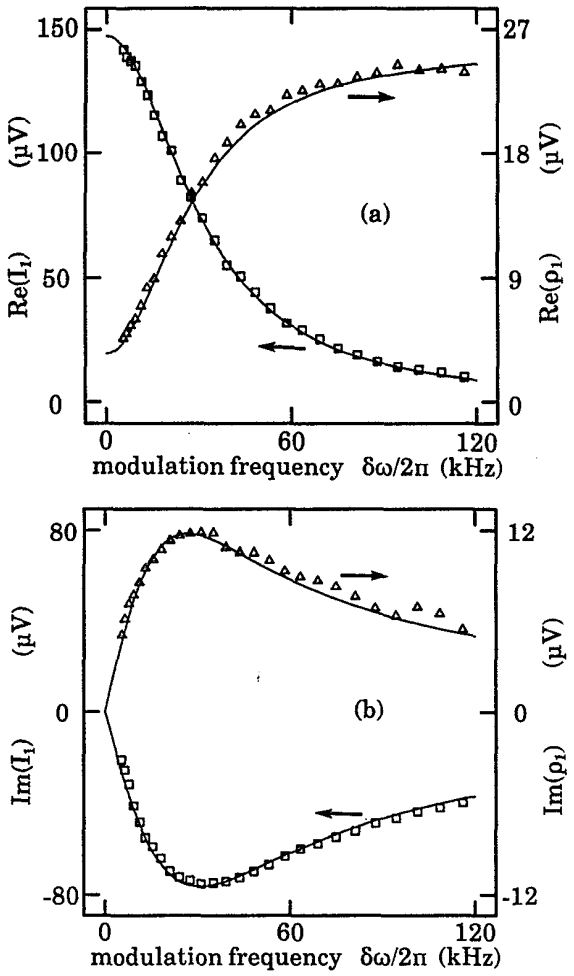

FIG. 11. (a) The in-phase first-harmonic response of the fluorescent intensity and the in-phase first-harmonic response of the laser intensity vs the modulation frequency $\delta\omega/2\pi$. We plot the in-phase first-harmonic response of the fluorescent intensity, triangles, and the in-phase first-harmonic response of the laser intensity, squares, for approximately the same pump parameter $\beta \simeq 0.018$. The solid lines represent the single-mode best theoretical fit to the data. (b) The in-quadrature first-harmonic response of the fluorescent intensity and the in-quadrature first-harmonic response of the laser intensity vs the modulation frequency $\delta\omega/2\pi$. We plot the in-quadrature first-harmonic response of the fluorescent intensity, triangles, and the in-quadrature first-harmonic response of the laser intensity, squares, for approximately the same pump parameter $\beta \simeq 0.018$. The solid lines represent the single-mode best theoretical fit to the data.

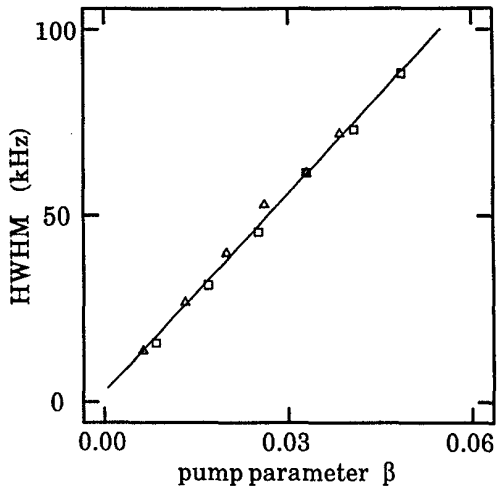

FIG. 12. The modulation bandwidth (HWHM) of the in-phase first-harmonic response of the fluorescent intensity and that of the in-phase first-harmonic response of the laser intensity vs the pump parameter β. The HWHM values of the curves shown in Figs. 9 and 10 are plotted. The HWHM values of the fluorescence curves are plotted using triangles and the HWHM values of the laser intensity curves are plotted using squares. The solid line represents the result of a linear regression performed on all the points shown. The slope of the line corresponds to a cavity lifetime of 90 ns.

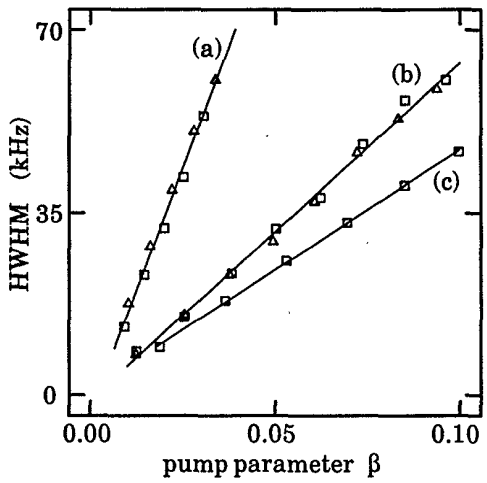

FIG. 13. The modulation bandwidth (HWHM) of the in-phase fluorescent and laser-intensity response vs the pump parameter β. The squares represent the dye-laser intensity response, the triangles represent the fluorescent intensity response, and the solid lines are lines resulting from linear regression analysis of these points. The cavities shown are (a) unidirectional ring cavity with 5% output coupler ($\tau_c = 85$ ns), (b) high-Q standing-wave cavity ($\tau_c = 246$ ns), and (c) high-Q bidirectional ring cavity ($\tau_c = 344$ ns).

back into the cavity. Retroreflection of one cavity direction is effective in providing unidirectional operation with an contrast ratio of at least 100:1 in these multimode lasers.

V. CONCLUSIONS

We employ AM spectroscopic techniques to study the effects of critical slowing down in a dye laser operating near the lasing threshold. We find that the total intensity of a multimode laser responds as a low-pass amplifier to pump modulations. This behavior is a manifestation of critical slowing down of the total intensity of a multimode laser operating near the lasing threshold. Our results show qualitative and quantitative agreement between multimode experiments and the predictions of single-mode laser theory. The fact that the total intensity of a multimode laser operating near threshold is well modeled by single-mode laser theory is an example of synergetic behavior in multimode lasers.[30] The many modes cooperate to maintain a total intensity which behaves according to single-mode laser theory, even though the underlying behavior of the individual modes is much more complicated.[31,32]

We qualify these conclusions by emphasizing that the lasers we studied were all extremely broadband. When the number of modes is not very large the modes may couple to produce deterministic oscillations of the total intensity of the laser in addition to the multiplicative fluctuations from the pump.[33] Another restriction which should apply to the interpretation of these results is that the modulation frequency was always much less than the free spectral range of the cavities. When the modulation frequency is comparable to the mode spacing and the modulation amplitude is large, the modes may couple to produce mode locking or deterministically chaotic fluctuations of the total intensity.[34–36] Furthermore, the gain medium in the dye-jet dye lasers we use in our experiments are extremely thin (i.e., 100 μm). A thin gain medium allows modes which differ substantially in frequency to maintain a constant phase difference throughout the gain medium, allowing many possible combinations of laser modes to uniformly saturate the gain medium. The laser cannot distinguish between the uniform saturation of many simultaneously lasing modes and a single traveling-wave mode.

We have also shown that the behavior of the atomic inversion in a laser gain medium displays some interesting dynamics. We measure the behavior of the excited-state population (this is equal to the inversion for an ideal four-level laser) in dye lasers by monitoring the intensity of the fluorescence emitted from the dye molecules in the gain region of the lasers. The response of the atomic inversion to pump modulations displays high-pass behavior. We interpret this result as evidence of low-frequency dynamic inversion clamping. Previously, inversion clamping has been interpreted as an adiabatic phenomenon.[31] In the presence of low-frequency pump fluctuations, the inversion remains constant while the system dissipates the absorbed pump fluctuations in the form of laser-intensity fluctuations. The laser intensity cannot follow high-frequency pump fluctuations; consequently, the inversion does not remain constant.

We apply these AM techniques to develop a novel method of determining the cavity lifetime. The cavity lifetime can be measured from AM frequency-domain measurements. This technique allows a modulator with small bandwidth to be used to measure a short cavity lifetime.

ACKNOWLEDGMENTS

The authors wish to acknowledge support of this research by the University Research Initiative through the U.S. Army Research Office and also Allied-Signal Corporation. Also we wish to express gratitude to Mark Beck and Ian McMackin for useful discussion of this work.

[1] K. Kaminishi, R. Roy, R. Short, and L. Mandel, Phys. Rev. A **24**, 370 (1981).
[2] R. Roy and L. Mandel, Opt. Commun. **34**, 133 (1980).
[3] P. Lett, E. C. Gage, and T. H. Chyba, Phys. Rev. A **35**, 746 (1987).
[4] P. Lett, Phys. Rev. A **34**, 2044 (1986).
[5] S. Zhu, A. W. Yu, and R. Roy, Phys. Rev. A **34**, 4333 (1986).
[6] S. N. Dixit and P. S. Sahni, Phys. Rev. Lett. **50**, 1273 (1983).
[7] R. Roy, A. W. Yu, and S. Zhu, Phys. Rev. Lett. **55**, 2794 (1985).
[8] R. J. Fox, Phys. Rev. A **34**, 3405 (1986).
[9] R. Graham, M. Höhnerbach, and A. Schenzle, Phys. Rev. Lett. **48**, 1396 (1982).
[10] A. Schenzle and R. Graham, Phys. Lett. **98A**, 319 (1983).
[11] R. F. Fox, G. E. James, and R. Roy, Phys. Rev. Lett. **52**, 1778 (1984).
[12] P. Jung and H. Risken, Phys. Lett. **103A**, 38 (1984).
[13] A. W. Yu, G. P. Agrawal, R. Roy, Opt. Lett. **12**, 806 (1987).
[14] G. P. Agrawal and R. Roy, Phys. Rev. A **37**, 2495 (1988).
[15] P. Mandel and T. Erneux, Phys. Rev. Lett. **53**, 1818 (1984).
[16] P. Mandel and T. Erneux, IEEE J. Quantum Electron. **QE-21**, 1352 (1985).
[17] G. Broggi, A. Colombo, L. A. Lugiato, and P. Mandel, Phys. Rev. A **33**, 3635 (1986).
[18] M. San Miguel and M. C. Torrent, J. Phys. (Paris) **49**, 149 (1988).
[19] M. C. Torrent and M. San Miguel, Phys. Rev. A **38**, 245 (1988).
[20] W. Scharpf, M. Squicciarini, D. Bromley, C. Green, J. R. Tredicce, and L. M. Narducci, Opt. Commun. **63**, 344 (1987).
[21] F. Papoff, D. Dangoisse, E. Poite-Hanoteau, and P. Glorieux, Opt. Commun. **67**, 358 (1988).
[22] F. Y. Wu, S. Ezekiel, M. Ducloy, and B. R. Mollow, Phys. Rev. Lett. **38**, 1077 (1977).
[23] L. W. Hillman, R. W. Boyd, J. Krasinski, and C. R. Stroud, Jr., Opt. Commun. **45**, 416 (1983).

[24]M. S. Malcuit, R. W. Boyd, L. W. Hillman, J. Krasinski, and C. R. Stroud, Jr., J. Opt. Soc. Am. B **1**, 73 (1984).
[25]M. A. Kramer, R. W. Boyd, L. W. Hillman, and C. R. Stroud, Jr., J. Opt. Soc. Am. B **2**, 1444 (1985).
[26]S. H. Chakmakjian, K. Koch, S. Papademetriou, and C. R. Stroud, Jr., J. Opt. Soc. Am. B (to be published).
[27]H. Fu and H. Haken, J. Opt. Soc. Am. B **5**, 899 (1988).
[28]H. Fu and H. Haken, Phys. Rev. Lett. **60**, 2614 (1988).
[29]A. E. Siegman, *Lasers* (University Science Books, California, 1986), Chap. 13.
[30]H. Haken, *Synergetics* (Springer-Verlag, New York, 1983).
[31]I. McMackin, C. Radzewicz, M. Beck, and M. G. Raymer, Phys. Rev. A **38**, 820 (1988).
[32]H. Atmanspacher, H. Scheingraber, and C. R. Vidal, Phys. Rev. A **33**, 1052 (1986).
[33]S. Chakmakjian, L. W. Hillman, K. Koch, and C. R. Stroud, Jr., *Optical Bistability III* (Springer-Verlag, New York, 1986).
[34]T. Ogawa and E. Hanamura, Opt. Commun. **61**, 49 (1987).
[35]T. Ogawa and E. Hanamura, Appl. Phys. B **43**, 139 (1987).
[36]T. Ogawa, Phys. Rev. A **37**, 4286 (1988).